Science Advances
AAAS

advances.sciencemag.org/cgi/content/full/6/13/eaay9789/DC1

# Supplementary Materials for

## Irradiated tumor cell–derived microparticles mediate tumor eradication via cell killing and immune reprogramming

Chao Wan, Yajie Sun, Yu Tian, Lisen Lu, Xiaomeng Dai, Jingshu Meng, Jing Huang, Qianyuan He, Bian Wu, Zhanjie Zhang, Ke Jiang, Desheng Hu, Gang Wu, Jonathan F. Lovell, Honglin Jin*, Kunyu Yang*

*Corresponding author. Email: yangky71@aliyun.com (K.Y.); jin@hust.edu.cn (H.J.)

Published 25 March 2020, *Sci. Adv.* **6**, eaay9789 (2020)
DOI: 10.1126/sciadv.aay9789

**The PDF file includes:**



**Other Supplementary Material for this manuscript includes the following:**

(available at advances.sciencemag.org/cgi/content/full/6/13/eaay9789/DC1)

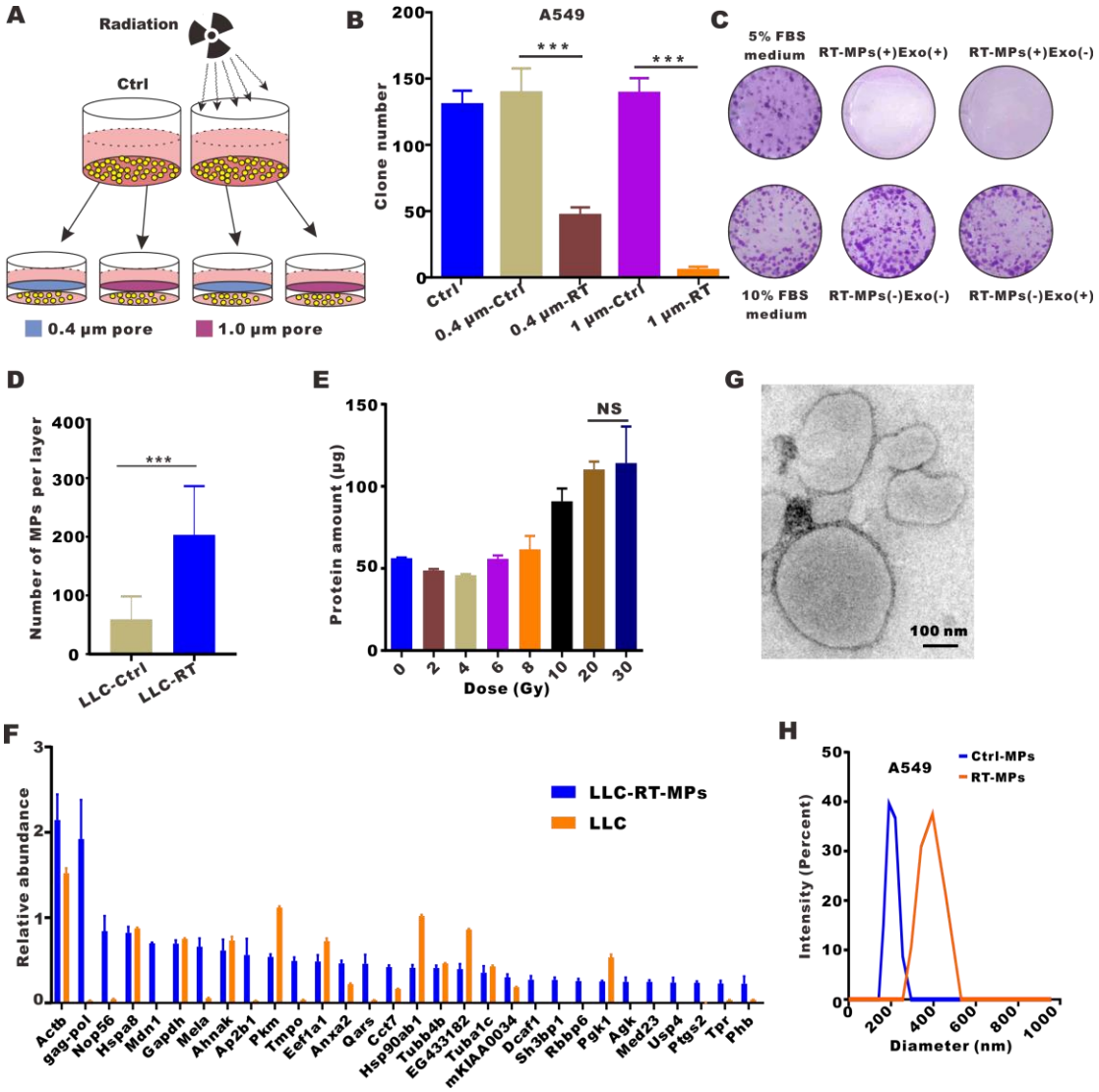


**Fig. S1. Examination of RIBE in irradiated A549 cells.** (**A**) Experimental outline for co-culturing with medium from irradiated cells using different pore sizes. (**B**) Clone numbers after co-culturing with medium from irradiated cells using 0.4 μm and 1 μm pores. (**C**) Representative images showing the colony numbers of A549 cells in the presence of microparticles or exosomes. (**D**) Quantitative analysis of red MPs in at least 10 fields of view ( n=3-4 per group). (**E**) Amounts of RT-MP production with various radiation doses. (**F**) Proteins in the top 30 of RT-MPs by proteomics. (**G**) TEM images of A549-derived RT-MPs (scale bar, 100 nm). (**H**) Representative sizes and particle distribution plots of A549-derived RT-MPs.

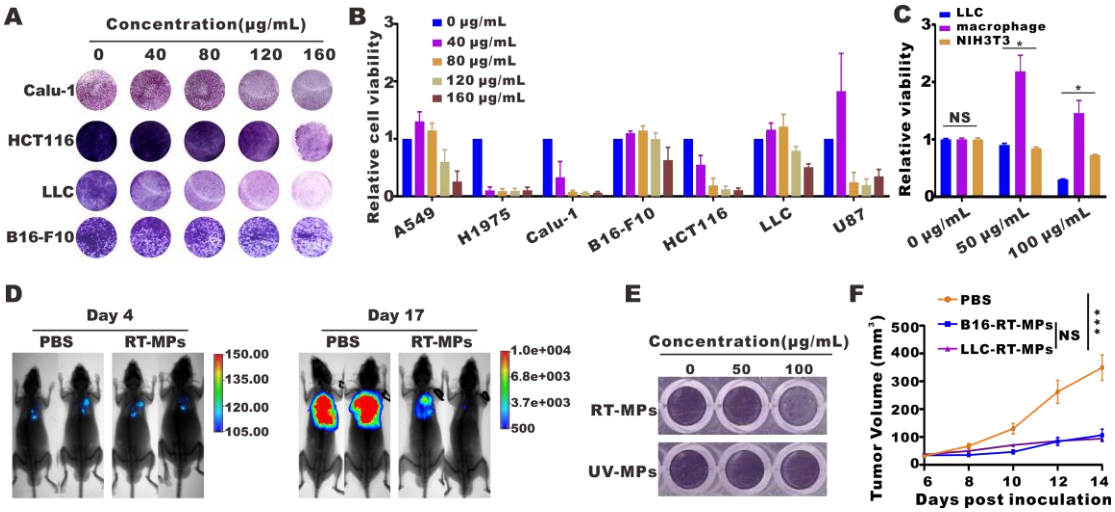


**Fig. S2. Therapeutic effect of RT-MPs.** (**A**) Calu-1, HCT116, LLC and B16-F10 cells were treated with different concentrations of RT-MPs (40, 80, 120, and 160 μg/mL) for 48 h. (**B**) A549-derived RT-MPs were added to other types of tumor cells. Cell viability was estimated using CCK-8 assays. (**C**) Lewis-derived RT-MPs were added to different cell. Cell viability was estimated using CCK-8 assays. (**D**) Representative *in vivo* bioluminescence images to detect the growth of thorax-injected Lewis-LUC cells in different groups of mice. (**E**) Lewis cells were treated with RT-MPs and UV-MPs in different concentration. (**F**) Tumor growth curves of B16-F10-LUC subcutaneous transplant model in corresponding treatment groups (n = 8-9 per group).

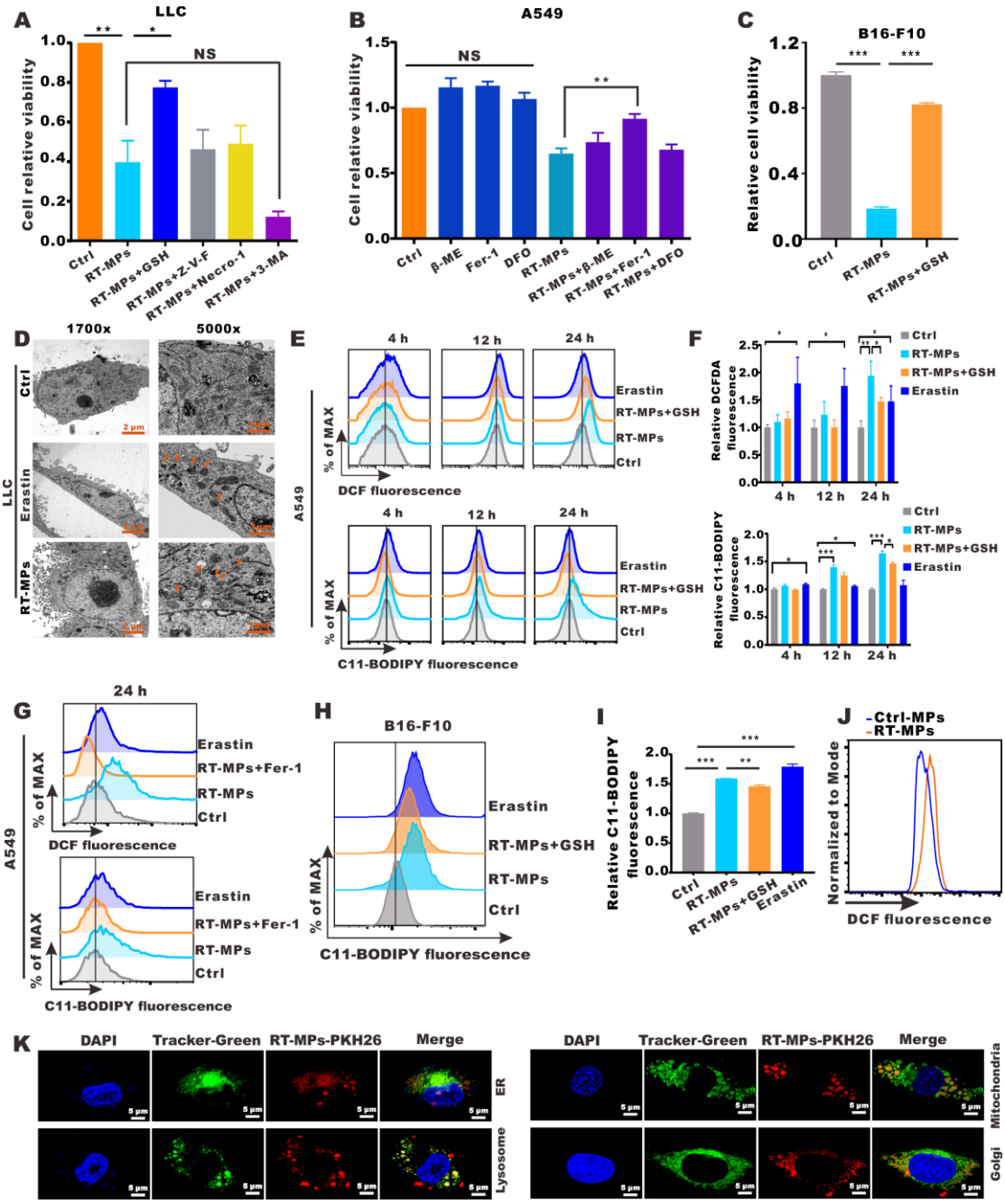


**Fig. S3. RT-MPs induce ferroptosis in tumor cells.** (**A**) Modulatory profiling of known small-molecule cell death inhibitors in Lewis cells treated with RT-MPs (100 μg/mL, 48 h). (**B**) Ferroptosis inhibitors were used in A549 cells treated with RT-MPs (100 μg/mL, 48 h). (**C**) L-GSH was used in B16-F10 cells treated with RT-MPs (100 μg/mL, 48 h). (**D**) Transmission electron microscopy of Lewis cells treated with PBS (24 h), elastin (2 μM, 24 h), and RT-MPs (100 μg/mL, 24 h). Single orange

arrowheads indicated shrunken mitochondria. At least 10 cells were examined in each treatment condition were examined. (**E**) Cytosolic and lipid ROS production assessed over time (4, 12, and 24 h) by flow cytometry using H2DCFDA and C11-BODIPY. (**F**) Quantification analysis of fig. S3E. (**G**) Cytosolic and lipid ROS production assessed by flow cytometry using H2DCFDA and C11-BODIPY. (**H** and **I**) Lipid ROS production assessed by flow cytometry using C11-BODIPY and its quantity analysis at 24h. (**J**) Cytosolic ROS in microparticles assessed by flow cytometry using H2DCFDA. (**K**) RT-MP membranes were not present in endoplasmic reticulum or Golgi apparatus, but showed enhanced colocalization with lysosomes and mitochondria in A549 cells. A549 cells were incubated with PKH26-labeled RT-MPs for 4 h, then analyzed with mitochondria, ER, Golgi and lysosome Green Trackers (scale bar, 5 μm).

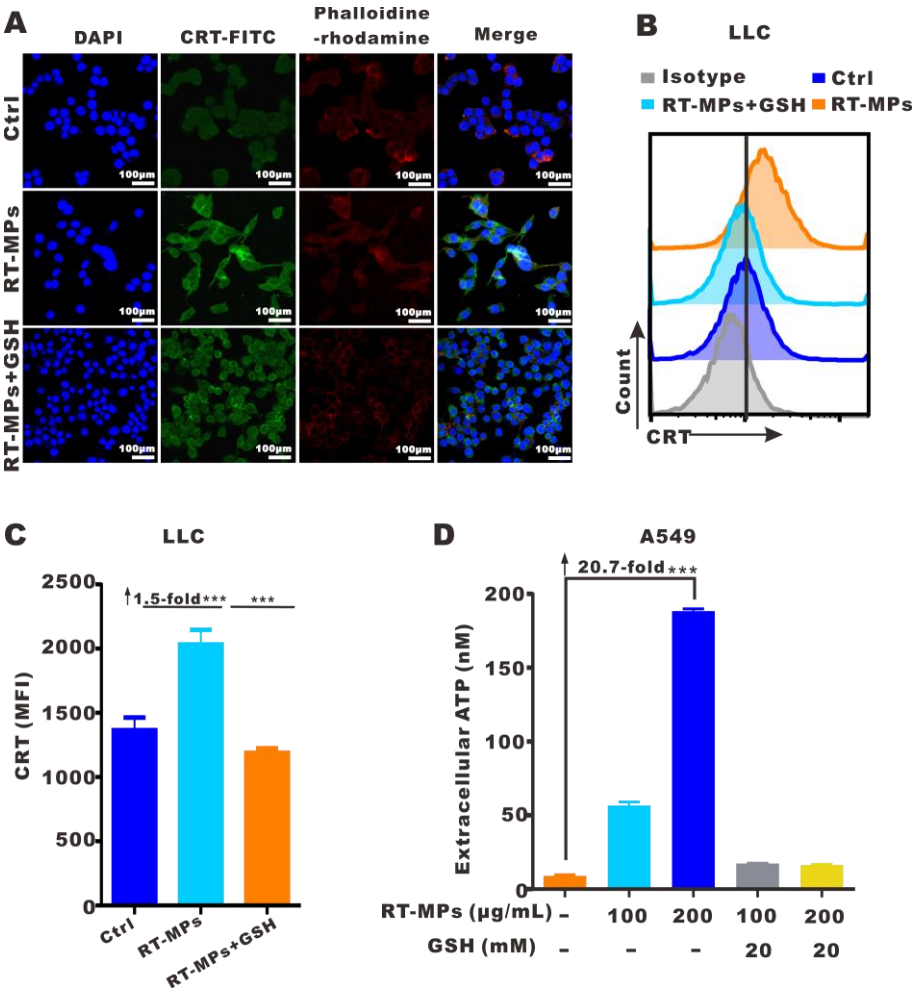


**Fig. S4. RT-MPs promote immunogenic cell death.** (**A**) Immunofluorescence staining of CRT expression (green) on surfaces of Lewis cells after various treatments. Phalloidine-rhodamine (red) represents the cytoskeleton. Scale bar, 100 μm. (**B-C**) Flow cytometric analysis of CRT expression level. (**D**) ATP levels in A549 cells treated with the indicated compounds.

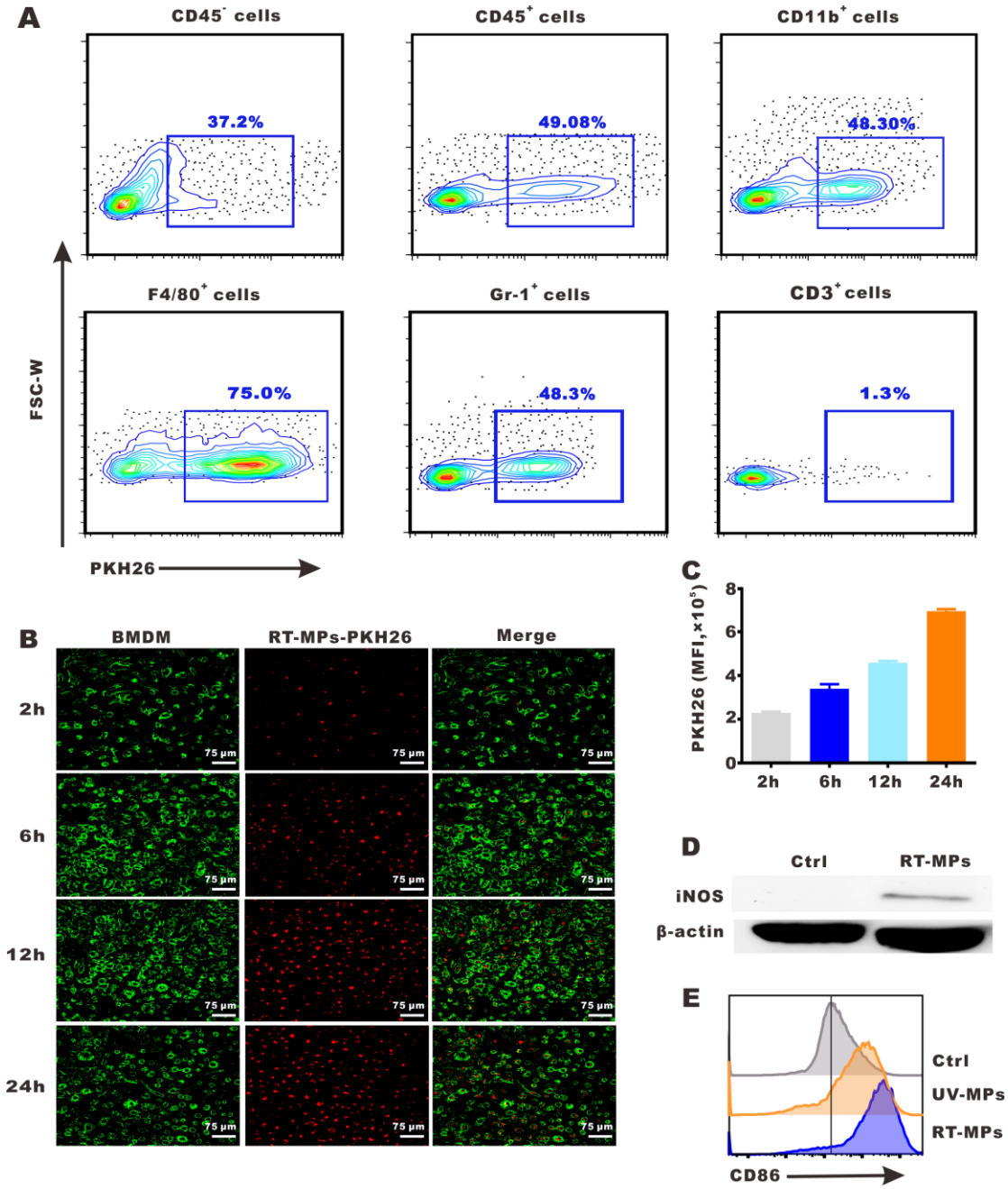


**Fig. S5. Macrophages show robust phagocytosis of RT-MPs.** (**A**) Representative flow cytometry dot plots of the accumulation of PKH67-labeled RT-MPs in lymphocytes and macrophages in MPE mice. (**B**) Confocal images revealed time-dependent accumulation of RT-MPs in macrophages. (**C**) Quantification of the phagocytosis of PKH26-labeled RT-MPs by macrophages. (**D**) The expression of iNOS, with or without RT-MP

treatment, was analyzed by western blotting. (**E**) Flow cytometric analysis of CD86 expression in BMDM-M2 cells treated with RT-MPs and UV-MPs.

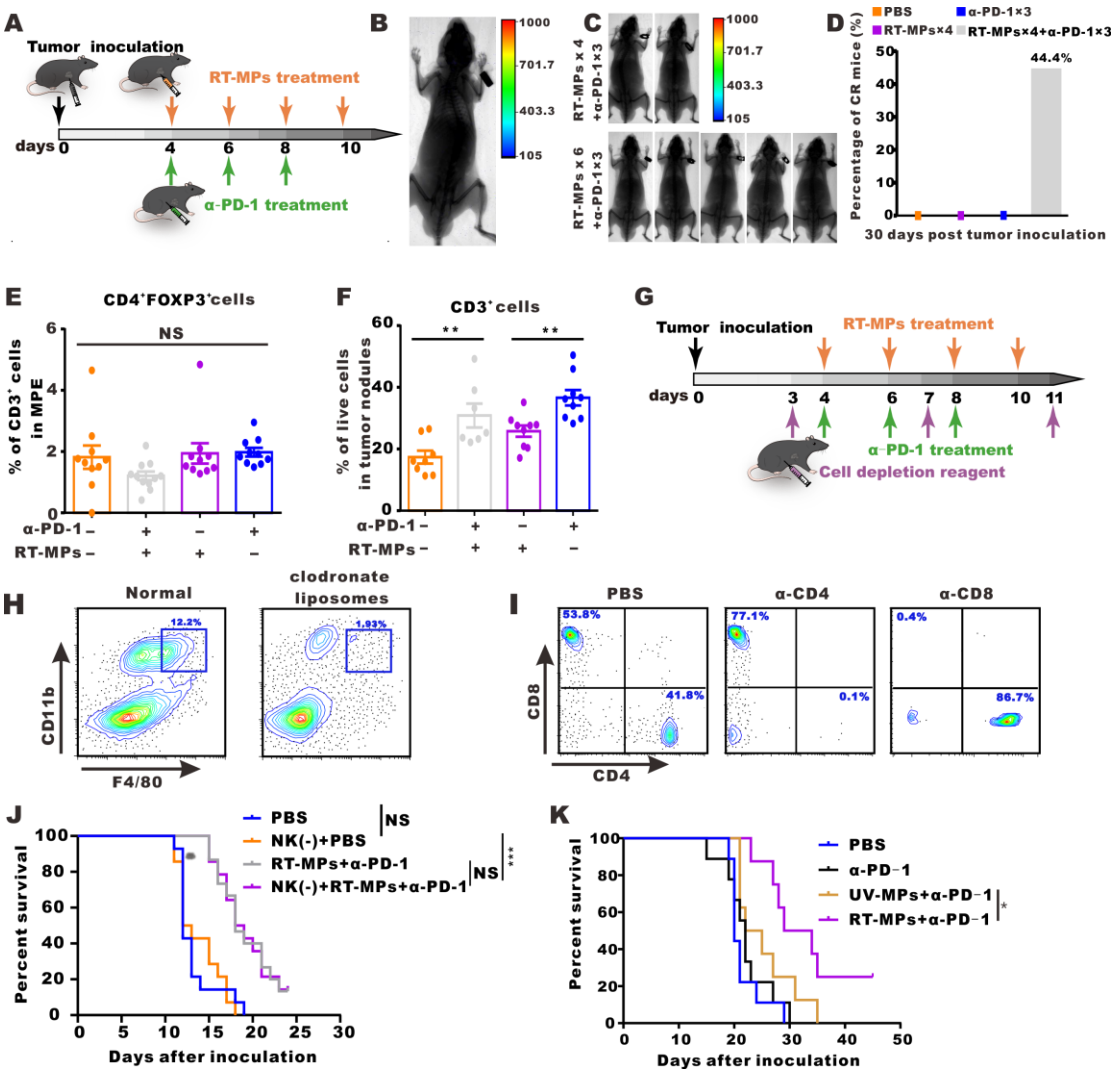


**Fig. S6. Therapeutic effect of combination treatment with RT-MPs and anti–PD-1 depends on immune system activation.** (**A**) Experimental outline for animal experiment. [ Picture by Chao Wan/Cancer center, Wuhan Union Hospital] (**B**) *In vivo* bioluminescence images to monitor the growth of the cured mouse in the combined group. (**C**) *In vivo* bioluminescence images to monitor the growth of the cured mice of different frequencies of RT-MP injection. (**D**) Percentages of mice with

complete response at 30 days after tumor inoculation in each group. (**E**) Percentages of $CD4^+FOXP3^+$ Treg cells among $CD3^+$ T cells from mice in each group. (**F**) Percentages of $CD3^+$ T cells among live cells in pleural solid tumors from mice in each group. (**G**) Experimental outline for depletion animal experiment. [ Picture by Chao Wan/Cancer center, Wuhan Union Hospital] (**H**) The numbers of $F4/80^{hi}$ and $CD11b^{hi}$ cells in the spleen of C57BL/6 mice were analyzed by flow cytometry after 2 days of treatment with or without 200 μL clodronate liposomes. (**I**) The numbers of splenic $CD4^+$ and $CD8^+$ T cells within the $CD3^+$ T cell gate in C57BL/6 mice were quantified by flow cytometry after 2 days of treatment with or without 200 μL anti-CD4 and anti-CD8 antibodies. (**J**) Kaplan–Meier survival plot of LLC-LUC MPE-bearing C57BL/6 mice treated with RT-MPs plus anti-PD-1, concomitant with NK 1.1 antibody treatment (n = 15 per group). (**K**) Kaplan–Meier survival plot of MPE mice in the corresponding treatment groups.

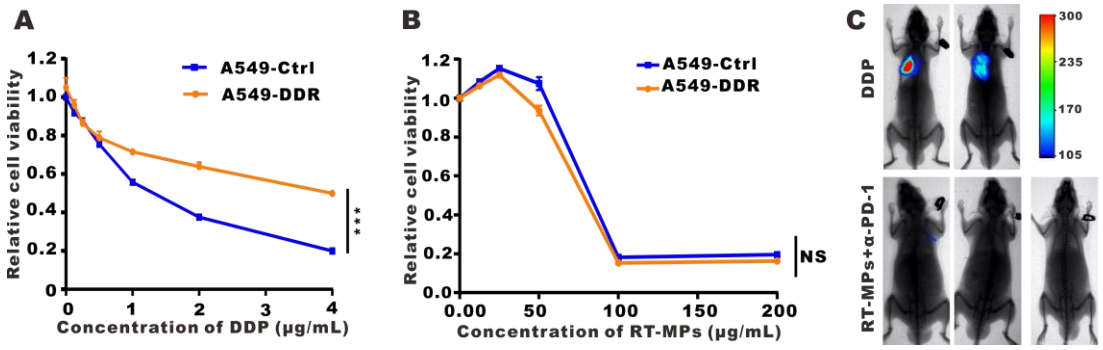


**Fig. S7. Therapeutic effect of RT-MPs on A549-DDR cells.** (**A**) Sensitivity of A549-Ctrl and A549-DDR cells to DDP. Relative cell viability was measured by CCK-8 assay. Error bars represent mean ± standard error of the mean. (**B**) Sensitivity of A549-Ctrl and A549-DDR cells to RT-MPs. Relative cell viability was measured by

CCK-8 assay. Error bars represent mean ± standard error of the mean. (**C**) Representative *in vivo* bioluminescence images to monitor the growth of thorax-injected Lewis-DDR cells in different groups of mice.

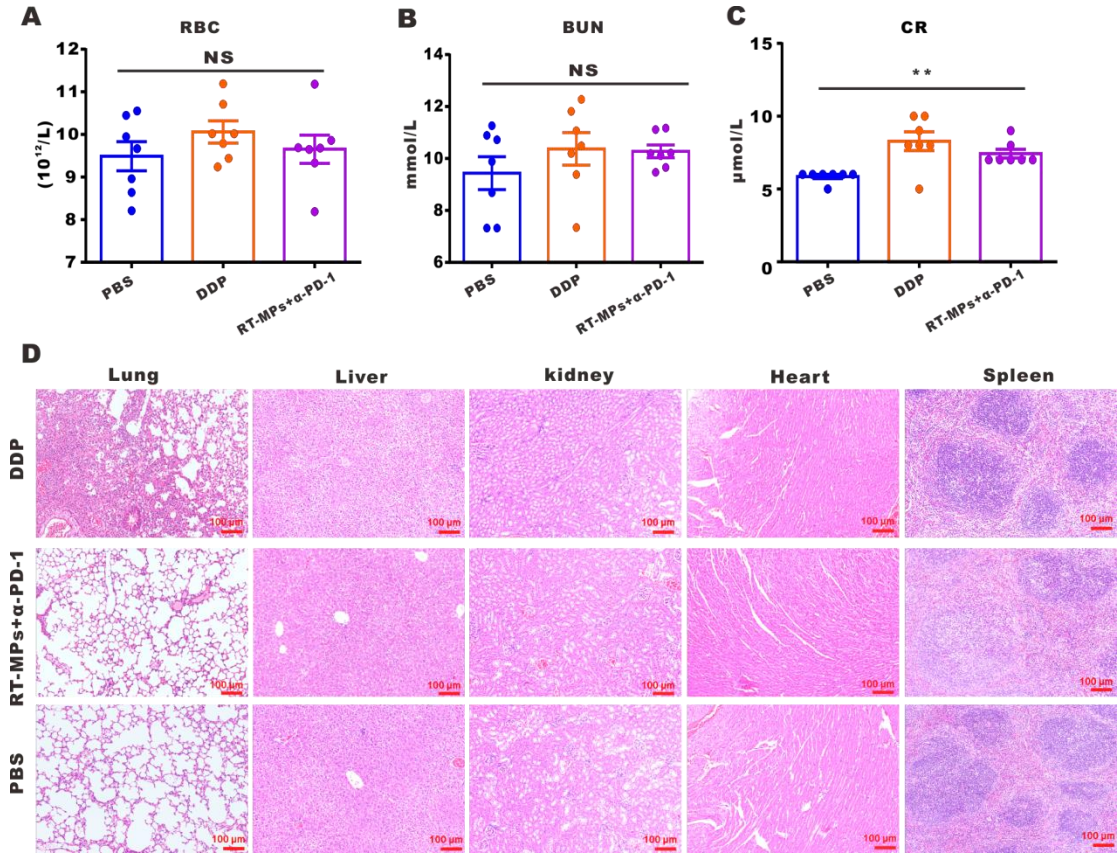


**Fig. S8. Hemanalysis and biochemical analyses.** (**A**) Hemanalysis was performed on blood withdrawn from mice on day 3 after treatment. RBC counts are presented as the mean ± standard error of the mean (n = 7). (**B** and **C**) Blood urea nitrogen and creatinine are presented as the mean ± standard error of the mean (n = 7). (**D**) Representative histological examinations of main organs with hematoxylin and eosin staining. Images of main organs from mice injected with PBS, RT-MPs plus anti-PD-1, or DDP (scale bar, 100 μm).

**Table S1. Sequences of primers for RT-qPCR analysis.**

| Gene name | Forward primer | Reverse primer |
|---|---|---|
| *Tnfα* | CATCTTCTCAAAATTCGAGTGACAA | TGGGAGTAGACAAGGTACAACCC |
| *Nos2* | CACCAAGCTGAACTTGAGCG | CCATAGGAAAAGACTGCACCG |
| *IL1* | ACCCCAAAAGATGAAGGGCTG | TACTGCCTGCCTGAAGCTCT |
| *IL6* | GAGGATACCACTCCCAACAGACC | AAGTGCATCATCGTTGTTCATACA |
| *IL10* | CAGAGAAGCATGGCCCAGA | TGCTCCACTGCCTTGCTCTTA |
| *IL12α* | CACCCTTGCCCTCCTAAACC | CACCTGGCAGGTCCAGAGA |
| *IL12p35* | GGAACTACACAAGAACGAGAG | AAGTCCTCATAGATGCTACCA |
| *IL12p40* | TGGTTTGCCATCGTTTTGCTG | ACAGGTGAGGTTCACTGTTTCT |
| *Ifnα* | TGATGGTCTTGGTGGTGAT | TTGTGCCAGGAGTGTCAA |
| *Ifnβ* | GGTGGAATGAGACTATGTTG | CTTCAAGTGGAGAGCAGTT |
| *TGFβ* | AACAATTCCTGGCGTTACCT | GGCTGATCCCGTTGATTTCC |
| *Chitinase* | CCCTGGGTCTCGAGGAAGCCC | GCAGCCTTGGAATGTCTTTCTCCAC |
| *Irf4* | GCCCAACAAGCTAGAAAG | TCTCTGAGGGTCTGGAAACT |

**Table S2. Antibodies used in this article.**

| Antibodies | source | detail information |
|---|---|---|
| CD9 | ABclonal | CD9 Monoclonal Antibody (A10789) |
| TSG101 | Abcam | Recombinant Anti-TSG101 antibody [EPR7130(B)] (ab125011) |
| i-NOS | CST | i-NOS Antibody (Mouse Specific) #2982 |
| p-p38 MAPK | CST | Phospho-p38 MAPK (Thr180/Tyr182) (D3F9) XP® Rabbit mAb #4511 |
| p-JNK | CST | Phospho-SAPK/JNK (Thr183/Tyr185) (81E11) Rabbit mAb #4668 |
| p-Erk1/2 | CST | Phospho-p44/42 MAPK (Erk1/2) (Thr202/Tyr204) (D13.14.4E) XP® Rabbit mAb #4370 |
| p-Stat1 | CST | Phospho-Stat1 (Ser727) (D3B7) Rabbit mAb #8826 |
| β-actin | ABclonal | ACTB Monoclonal Antibody (AC026) |
| Anti-CRT | Abcam | Recombinant Anti-Calreticulin antibody [EPR3924] - ER Marker (ab92516) |
| Second antibody | Proteintech | HRP-conjugated Affinipure Goat Anti-Rabbit IgG(H+L) #SA00001-2 |